J Supercond Nov Magn (2015) 28:1065–1070
DOI 10.1007/s10948-014-2892-6

ORIGINAL PAPER

Structural, Magnetic and Magnetocaloric Study of Polycrystalline $(1-x)La_{0.65}Ca_{0.35}MnO_3/xCr_2O_3$ Composites

A. Marzouki-Ajmi · W. Cheikhrouhou-Koubaa · M. Koubaa · A. Cheikhrouhou

Received: 11 November 2014 / Accepted: 14 November 2014 / Published online: 26 November 2014

Abstract Magnetic and magnetocaloric properties of polycrystalline $(1-x)La_{0.65}Ca_{0.35}MnO_3/xCr_2O_3 (0 \leq x \leq 0.3)$ composites were investigated. Our composites were elaborated using the solid-state reaction at high temperature. Polycrystalline $La_{0.65}Ca_{0.35}MnO_3$ (LCMO) was synthesized using the solid-state reaction at high temperature while for Cr_2O_3 we used a commercial product. X-ray diffraction patterns show that the parent compound $La_{0.65}Ca_{0.35}MnO_3$ is single phase without any detectable impurity and crystallizes in the orthorhombic structure with *Pbnm* space group. Magnetocaloric effect of our composite materials in the vicinity of the magnetic transition temperatures was investigated. The maximum of the magnetic entropy change $|\Delta S_M^{max}|$ is found to be 5.5, 5.12, 4.5, and 3.12 J kg^{-1} K^{-1} for $x = 0, 0.1, 0.2,$ and 0.3 under a magnetic field change of 5 T, respectively.

Keywords Manganites · Composites · Electron microscopy · Magnetic entropy change

1 Introduction

Nowadays, the search for new materials with enhanced magnetocaloric effect (MCE) for their utilization in room temperature magnetic refrigerators is a very active field of research due to its lower energy consumption and environmental-friendly character. The magnetocaloric effect was first discovered by Warburg in 1881 [1], Deby in 1926 [2], and Giauque in 1927 [3] independently pointed out that ultra-low temperature could be reached through the reversible temperature change of paramagnetic salts with the alternation of magnetic field and first foresaw the technological potential of this effect. Magnetic refrigeration near room temperature is of special interest because of its great social effect and economical benefit. The prototype magnetic material available for room temperature magnetic refrigeration is gadolinium Gd. At the Curie temperature T_C of 294 K, Gd undergoes a second-order paramagnetic–ferromagnetic transition. The MCE and the heat capacity of Gd have been studied in many research activities [4]. Recently, large values of MCE are observed in the perovskite manganese oxides [5–10]. The research is very interesting in the system $La_{1-x}Ca_xMnO_3$ which is characterized by rather large values of MCE and adjustable phase transition temperatures [5, 11–13]. For $La_{0.65}Ca_{0.35}MnO_3$ elaborated using the solid–solid reaction method at high temperature, the $|\Delta S_M^{max}|$ under an applied field of 5 T reaches 5.5 J kg^{-1} K^{-1}, around its Curie temperature $T_C = 265$ K [14]. Moreover, the presence of magnetic multiphases broadens the $\Delta S_M(T)$ curves and enhances consequently the relative cooling power (RCP) [15–20]. In this context, several magnetocaloric studies have been performed recently on composites based on manganites in order to enhance the physical properties comparing to manganites [21–25]. In our study, we elaborated polycrystalline composites based on $La_{0.65}Ca_{0.35}MnO_3$ manganites with Cr_2O_3 oxide at several mass fractions and studied their magnetic and magnetocaloric properties of $(1–x)La_{0.65}Ca_{0.35}MnO_3/xCr_2O_3$ with $x=0, 0.1, 0.2,$ and 0.3.

A. Marzouki-Ajmi · W. Cheikhrouhou-Koubaa (✉) · M. Koubaa · A. Cheikhrouhou
Laboratoire de Physique des Matériaux, Faculté des Sciences de Sfax, Sfax University, B.P. 1171, 3000 Sfax, Tunisia
e-mail: wissem.koubaa@yahoo.fr

A. Cheikhrouhou
Centre de Recherche en Informatique, Multimédia et Traitement Numérique des Données, Sfax Technoparc, B.P 275, 3029 Sfax, Tunisia

2 Experiments

2.1 Synthesis

The composites $(1-x)La_{0.65}Ca_{0.35}MnO_3/xCr_2O_3$ ($x = 0$, 0.1, 0.2, and 0.3) were synthesized in two stages. First, we elaborated $La_{0.65}Ca_{0.35}MnO_3$ sample using the ceramic route at high temperatures, stoichiometric amounts of dried La_2O_3, $CaCO_3$, and MnO_2, with high purity equal to 99.9 %, according to the following equation:

$$0.325La_2O_3 + 0.35CaCO_3 + MnO_2 \rightarrow La_{0.65}Ca_{0.35}MnO_3 + \delta CO_2 + \delta' O_2$$

were intimately mixed in an agate mortar for 45 min; the obtained powder was pressed into pellets of about 1 mm thickness and 13 mm diameter and sintered at 1000 °C in air for 24 h. The sample undergoes several cycles of grinding–pelleting–annealing between 1000 and 1200 °C during 48 h for each annealing. The obtained sample was characterized by X-ray powder diffraction at room temperature with CuKα radiation. Structural analysis was made using the standard Rietveld technique [26, 27]. Secondly, we have prepared three composites based on $La_{0.65}Ca_{0.35}MnO_3$ and Cr_2O_3 for different mass fractions. The composites were prepared by thoroughly mixing 90, 80, and 70 % of $La_{0.65}Ca_{0.35}MnO_3$ with 10, 20, and 30 % of Cr_2O_3, respectively, and then were sintered at 1000 °C for 4 h. The microstructure was studied by scanning electron microscope (SEM). The density of the as-produced pellets was measured with a Micromeritics AccuPyc 1330 helium pycnometer. Magnetization measurements versus magnetic applied field up to 5 T were performed using a vibrating sample magnetometer in the temperature range 200–350 K., Magnetocaloric effect $|\Delta S_M(T)|$ at several magnetic field change up to 5 T were deduced from the $M(H)$ curves at several temperatures.

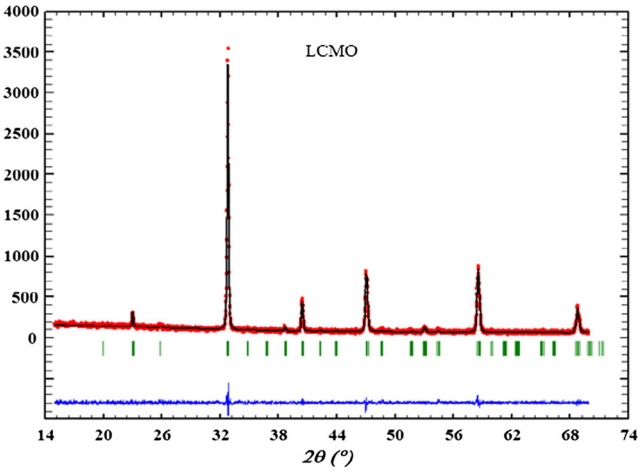

Fig. 1 X-ray diffraction patterns at 300 K for $La_{0.65}Ca_{0.35}MnO_3$ sample including the observed and calculated profiles as well as the difference profile

3 Results and Discussion

The X-ray diffraction (XRD) patterns of the parent compound $La_{0.65}Ca_{0.35}MnO_3$ have been recorded at room temperature; the data have been refined using Rietveld's profile-fitting method. Figure 1 shows the X-ray diffraction patterns at 300 K for $La_{0.65}Ca_{0.35}MnO_3$ sample including the observed and calculated profiles as well as the difference profile. Our parent compound is single phase without any detectable impurity and crystallizes in the orthorhombic structure with *Pbnm* space group. Figure 2 shows the X-ray diffraction patterns at 300 K for our three composites $(1-x)La_{0.65}Ca_{0.35}MnO_3/xCr_2O_3$ with $x = 0.1$, 0.2, and 0.3. As we can observe in this figure, there is no interaction between the parent compound and Cr_2O_3 oxide.

3.1 Microstructural Analysis

To investigate the microstructural properties of our synthesized samples XRD and SEM analyses were jointly used. With MAUD software, the model line broadening selected was "popa LB" combined with the isotropic model size strain. The instrument broadening was corrected using the XRD pattern of a Si standard. Figure 3 shows the SEM image obtained for the composites $(1-x)La_{0.65}Ca_{0.35}MnO_3/xCr_2O_3$, ($x = 10$ and 30 %). The SEM image shows that the Cr_2O_3 oxide occupies the grain boundary of $La_{0.6}Ca_{0.35}MnO_3$.

3.2 Magnetic and Magnetocaloric Properties

We performed magnetization measurements versus magnetic applied field up to 5 T at several temperatures in the range 200–350 K for the parent

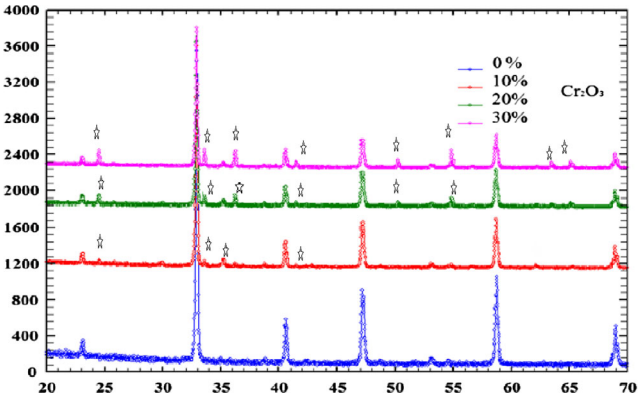

Fig. 2 X-ray diffraction patterns at 300 K for LSMO and the three composites $(1-x)La_{0.65}Ca_{0.35}MnO_3/xCr_2O_3$ with $x = 0.1$, 0.2, and 0.3

compound $La_{0.65}Ca_{0.35}MnO_3$ and the three composites $(1-x)La_{0.65}Ca_{0.35}MnO_3/xCr_2O_3$ ($x = 10$, 20, and 30 %). Figure 4 shows the magnetic field dependence of magnetization up to 5 T at several temperatures $(1-x)La_{0.65}Ca_{0.35}MnO_3/xCr_2O_3$ ($x = 10$ and 20 %). At low temperatures, the magnetization M increases sharply with magnetic applied field for $H < 0.5$ T and then saturates above 1 T. This result confirms well the ferromagnetic behavior at low temperatures of our composites. The hysteresis cycles exhibit a sigmoidal shape; this is due to the presence of structural distortions inside the grains. The small hysteresis losses are properties generally desired in soft magnetic materials. Figure 5 shows the hysteresis cycles for $(1-x)La_{0.65}Ca_{0.35}MnO_3/xCr_2O_3$ ($x = 10$, 20, and 30 %) at different temperatures. The different values of the coercivity and the saturated magnetization for our composites are summarized in Table 1. The magnetic entropy change $\Delta S_M(T)$ has been deduced from the isothermal magnetization measurements. It can be evaluated according to Maxwell's relations, using the following equation:

$$\Delta S_M(T, H) = S_M(T, H) - S_M(T, 0) = \int_0^{H_{\max}} \left(\frac{\partial M}{\partial T}\right)_H dH \quad (1)$$

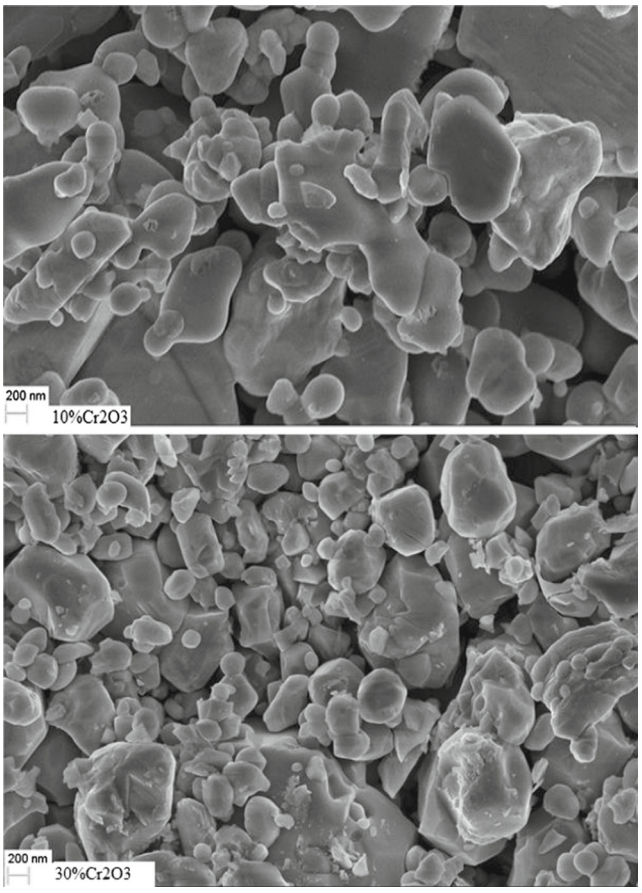

Fig. 3 SEM images of $(1-x)La_{0.65}Ca_{0.35}MnO_3/xCr_2O_3$ for $x = 10$ and 30 %

where $H_{\max}$ is the maximal value of the magnetic applied field. In practice, the relation is approximated as [19, 20]

$$\Delta S_M(T, H) = \sum_i \frac{M_{i+1}(T_i, H) - M_i(T_i, H)}{T_{i+1} - T_i} \Delta H_i \quad (2)$$

where M_i and M_{i+1} are the experimental values of magnetization measured at temperatures T_i and T_{i+1}, respectively, under a magnetic field H_i. Figure 6 shows the variation of $-\Delta S_M$ as a function of temperature at different magnetic field changes for our composites. As expected, $-\Delta S_M$ reaches its maximum around the transition temperature and increases with the magnetic applied field change. At 5 T, the maximal value of the magnetic entropy change $|\Delta S_M^{\max}|$ is found to be 5.5, 5.12, 4.5, and 3.12 J kg^{-1} K^{-1} for $x = 0$, 0.1, 0.2, and 0.3, respectively. We do not notice a significant effect of the mass fraction of Cr_2O_3 oxide on the maximum of $\Delta S_M(T)$ while temperature of this maximum is shifted to higher values. From a cooling perspective, it is important to consider the refrigeration capacity which depends on

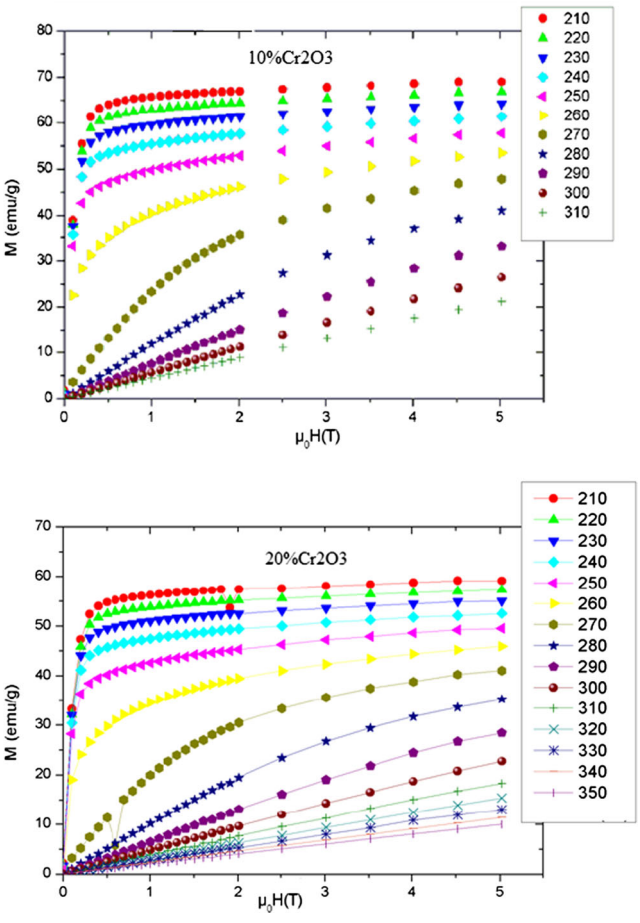

Fig. 4 Magnetic field dependence of magnetization up to 5T at several temperatures of $(1-x)La_{0.65}Ca_{0.35}MnO_3/xCr_2O_3$ with $x = 0.1$ and 0.2

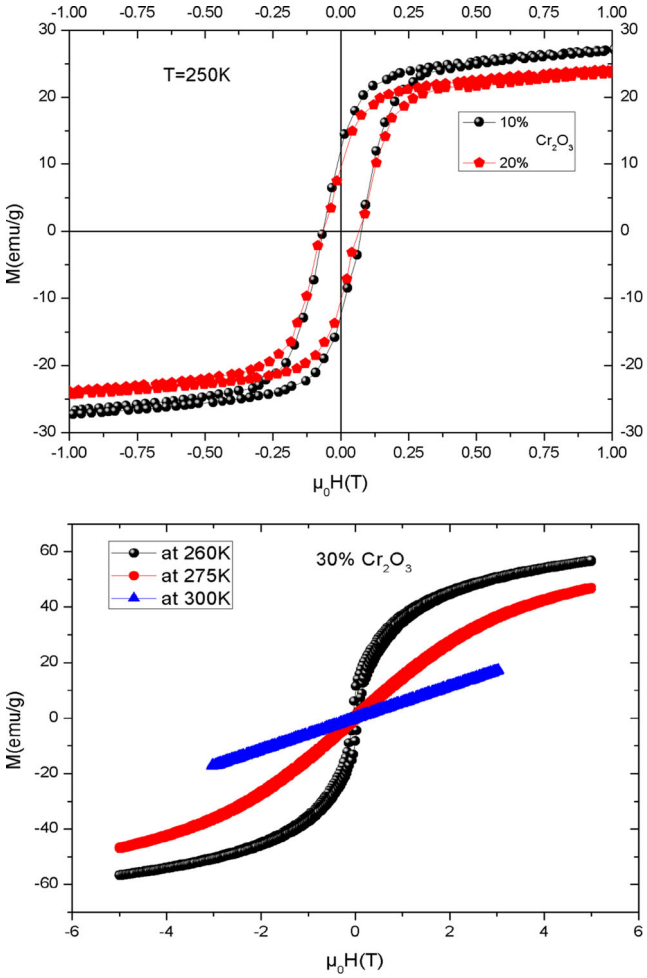

Fig. 5 Hysteresis of $(1-x)La_{0.65}Ca_{0.35}MnO_3/xCr_2O_3$ for $x = 10$, 20, and 30 % at different temperatures

both the magnetic entropy change and its temperature. The magnetic cooling efficiency of a magnetocaloric material can be evaluated through the relative cooling power (RCP) defined as

$$\mathrm{RCP} = \left|\Delta S_M^{\max}\right| \times \delta T_{\mathrm{FWHM}} \tag{3}$$

were δT_{FWHM} is the full with at half maximum of the $\Delta S_M(T)$ curve. The RCP value is found to be 238.3, 227.4, 193.7, and 145.1 J kg^{-1} for $x = 0$, 10, 20, and 30 %,

Table 1 Different values of the coercivity and the saturation magnetization of $(1-x)La_{0.65}Ca_{0.35}MnO_3/xCr_2O_3$ for $x = 10$, 20, and 30 % at 250, 260, and 275 K

T (K)	250		260
$\%Cr_2O_3$	10 %	20 %	30 %
$H_C(T)$	0.07	0.07	0.07
M_R(emu/g)	10.07	13.44	9.02

respectively, under a magnetic field change of 5 T. The RCP decreases with increasing the Cr_2O_3 amount in our composites. In this work, we have used the Landau theory of phase transitions to modelize the magnetocaloric effect in

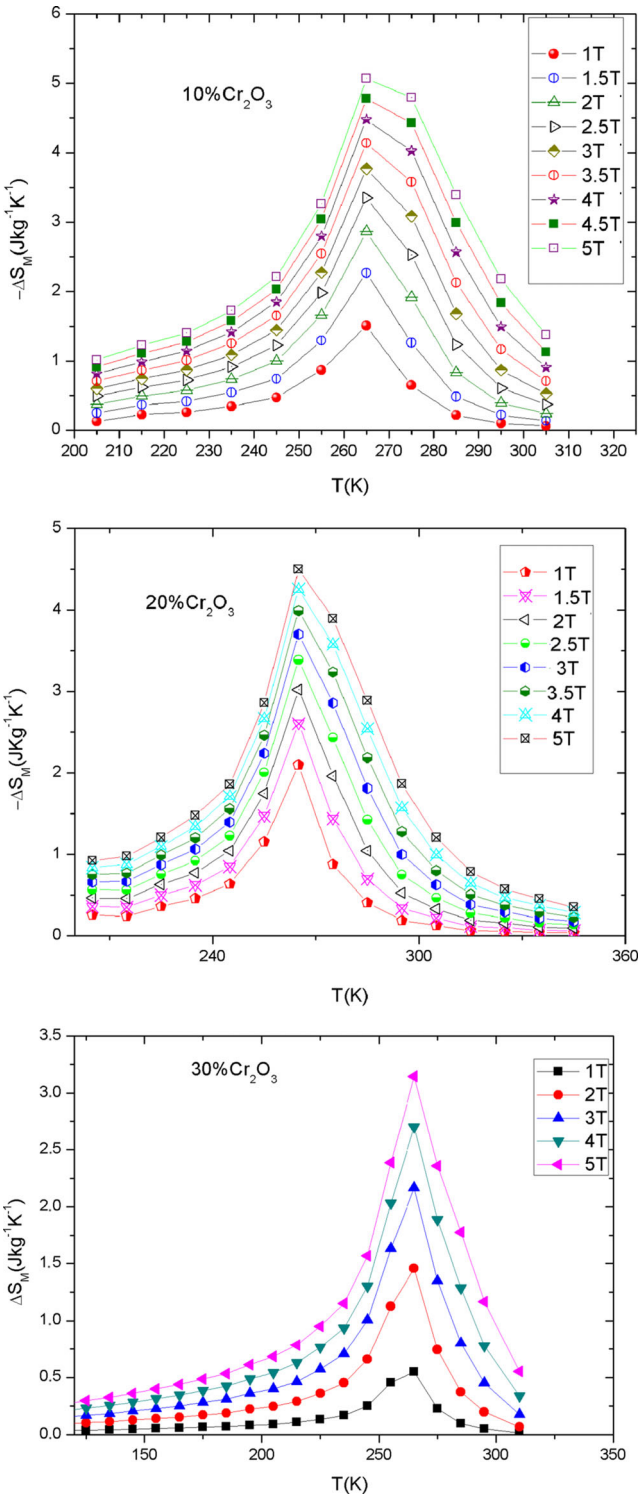

Fig. 6 Temperature dependence of the magnetic entropy change, $-\Delta S_M$, for different magnetic field changes for our composites

ferromagnetic materials [28]. In a recent framework, Gibbs free energy can be expressed by

$$G(M,T) = G_0 + \frac{1}{2}A(T)M^2 + \frac{1}{4}B(T)M^4 + \frac{1}{6}C(T)M^6 - MH \quad (4)$$

where the coefficients A, B, and C are temperature-dependent parameters usually known as Landau coefficients. For energy minimization in Eq. 4, the equation of state is given by

$$\frac{H}{M} = A(T) + B(T)M^2 + C(T)M^4 \quad (5)$$

The corresponding magnetic entropy is obtained from differentiation of the magnetic part of the free energy with respect to temperature

$$S(T,H) = -\frac{1}{2}A'(T)M^2\frac{1}{4} + B'(T)M^4 + \frac{1}{6}C'(T)M^6 \quad (6)$$

$A'(T)$, $B'(T)$, and $C'(T)$ are the temperature derivatives of the expansion coefficients. The same result is obtained using the equation of state and the integration of Maxwell relations. Nevertheless, in order to compare with the magnetic entropy change ($\Delta S(T,\mathrm{H})$) obtained for experimental measurements, we should also calculate the temperature dependence of the magnetic entropy without magnetic field $S(T, H = 0)$. Therefore, the theoretical magnetic entropy change $\Delta S(T, H)$ is

$$\Delta S(T,H) = -\frac{1}{2}A'(T)\left(M_0^2 - M^2\right) - \frac{1}{4}B'(T)\left(M_0^4 - M^4\right) - \frac{1}{6}C'(T)\left(M_0^6 - M^6\right) \quad (7)$$

Here, the value of M_0 can be obtained by extrapolating the magnetization at $H = 0$. As shown in Fig. 7, the circles represent the calculated magnetic entropy change by using Eq. 7 and the squares represent the experimental data. V.S Amaral and J.S Amaral [28] showed that the nature of the parameter $B(T)$ takes an important role in determining $\Delta S(T, H)$. For LCMO +30 % Cr_2O_3, $B(T)$ is observed to be negative below T_C and positive above T_C. This change from negative to positive suggests that the phase transition in the sample is of second order [29]. $B(T)$ parameter increases with temperature ($B' = dB/dT > 0$), the magnetic entropy is then larger and the peak broadened [28]. The variations of $A(T)$, $B(T)$, and $C(T)$ values for LCMO + 30 % Cr_2O_3 are shown in the inset of Fig. 7. It may be seen that the agreement between the theoretical and the measured data is very satisfactory, considering the fact that the present model does not take into account the influence of the Jahn–Teller effect and the exchange interactions on the magnetic properties of manganites. Nevertheless, the analysis clearly demonstrates the importance of magnetoelastic coupling and electron interaction in understanding the magnetocaloric properties of lanthanum manganites.

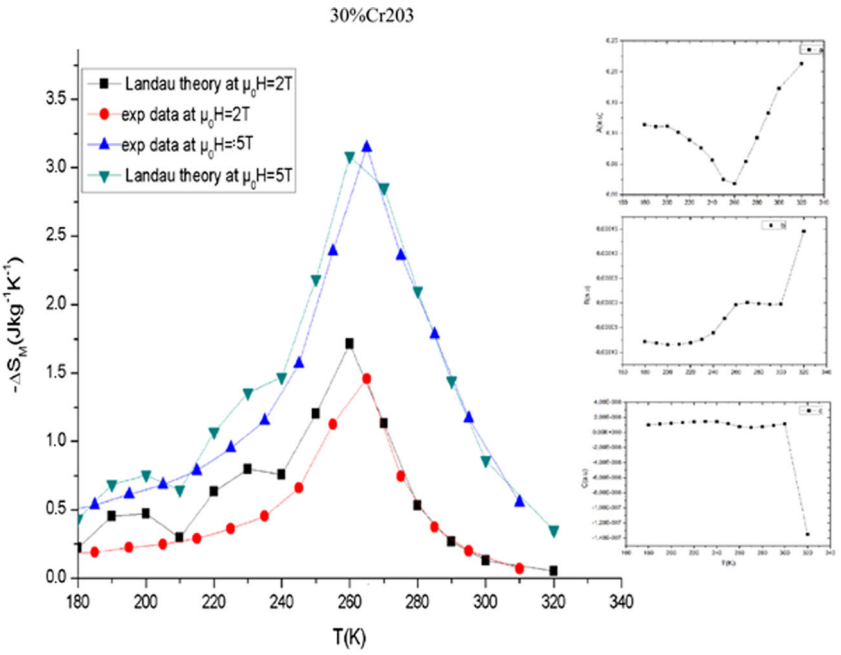

Fig. 7 Experimental and theoretical magnetic entropy change, $-\Delta S_M$, for $x = 30$ % Cr_2O_3 at $\Delta H = 2$ and 5 T. The *insets* show the temperature dependence of Landau coefficients $A(T)$, $B(T)$, and $C(T)$. The units for $A(T)$, $B(T)$, and $C(T)$ are $T^2\ kg^{-1}J^{-1}$, $T^4\ kg^{-3}\ J^{-3}$, and $T^6\ kg^{-5}\ J^{-5}$, respectively

4 Conclusion

We can observe from DRX diffractograms that Cr_2O_3 does not react with the parent compound, and it forms a secondary phase located on the grain boundaries, as revealed from SEM images. The Cr_2O_3 slightly affects both T_C and $|-\Delta S_M|$, but it induces a decrease in the remanent magnetization.

Acknowledgments This work has been supported by the Tunisian Ministry of Higher Education, Scientific Research and information and communication technology.

References

1. Warburg, E.: Ann. Phys. **13**, 141 (1881)
2. Debye, P.: Ann. Phys. **81**, 1154 (1926)
3. Giauque, W.F.: J. Am. Chem. Soc. **49**, 1864 (1927)
4. Yu, B.F., Gao, Q., Zhang, B., Meng, X.Z., Chen, Z.: Int. J. Refrig. **26**, 622 (2003)
5. Zhensheng, P.: J. Rare Earths **22**, 232 (2004)
6. Gschneidner, K.A. Jr., Pecharsky, V.K., Tsokol, A.O.: Rep. Prog. Phys. **68**, 1479 (2005)
7. Cheikhrouhou-Koubaa, W., Koubaa, M., Cheikhrouhou, A.: J. Alloys Compd. **470**, 42 (2009)
8. Koubaa, M., Cheikhrouhou-Koubaa, W., Cheikhrouhou, A.: J. Phys. Chem. Solids **70**, 326 (2009)
9. Cheikhrouhou-Koubaa, W., Koubaa, M., Cheikhrouhou, A.: J. Phys. Procedia **2**, 989 (2009)
10. Phan, M.H., Yu, S.C.: J. Magn. Magn. Mat. **308**, 325 (2007)
11. Schiffer, P.E., Ramirez, A.P., Bao, W., Cheong, S.W.: Phys. Rev. Lett. **75**, 3336 (1995)
12. Tang, W., Lu, W., Luo, X., Wang, B., Zhu, X., Song, W., Yang, Z., Sun, Y.: J. Magn. Magn. Mat. **322**, 2360 (2010)
13. Krichene, A., Boujelben, W., Cheikhrouhou, A.: J. Alloys Compd. **550**, 75 (2013)
14. Koubaa, M., Cheikhrouhou-Koubaa, W., Cheikhrouhou, A., Haghiri-Gosnet, A.M.: J. Phys. B **403**, 2477 (2008)
15. Caballero-Flores, R., Franco, V., Conde, A., Knipling, K.E., Willard, M.A.: Appl. Phys. Lett. **98**, 102505 (2011)
16. Smaili, A., Chahine, R.: Appl. Phys. Lett. **81**, 824 (1997)
17. de Oliveira, I.G., Von Ranke, P.J., Nobrega, E.P.: J. Magn. Magn. Mat. **261**, 112 (2003)
18. Chaturvedi, A., Stefanoski, S., Phan, M.H., Nolas, G.S., Srikanth, H.: Appl. Phys. Lett. **99**, 162513 (2011)
19. Paticopoulos, S.C., Caballero-Flores, R., Franco, V., Blasquer, J.S., Conde, A., Knipling, K.E., Willard, M.A.: Solid State Commun. **152**, 1590 (2012)
20. Romero Muniz, C., Franco, V., Conde, A.: Appl. Phys. Lett. **102**, 082402 (2013)
21. Pekala, M., Pekala, K., Drozd, V., Staszkie Wicz, K., Fagnard, J.F., Vanderbemden, P.: J. Appl. Phys. **112**, 023906 (2012)
22. Panwar, N., Coondoo, I., Agarwal, S.K.: Mater. Lett. **64**, 2638 (2010)
23. Lim, S.P., Tang, G.D., Li, Z.Z., Qi, W.H., Ji, D.H., Li, Y.F., Chen, W., Hou, D.L.: J. Alloys Compd. **509**, 2320 (2011)
24. Yang, H., Cao, Z.E., Shen, X., Xian, T., Feng, W.J., Jiang, J.L., Feng, Y.C., Wei, Z.Q., Dai, J.F.: J. Appl. Phys. **106**, 104317 (2011)
25. Yuan, G.L., Liu, J.M., Liu, Z.G., Du, Y.W., Chan, H.L.W., Choy, C.L.: Mater. Chem. Phys. **75**, 161 (2002)
26. Rietveld, H.M.: J. Appl. Cryst. **2**, 65 (1969)
27. Roisnel, T., Rodriguez-Carvayal, J.: Computer progasm Fullprof, LLB-LCSIM, May (2003)
28. Amaral, V.S., Amaral, J.S.: J. Magn. Magn. Mater. **272–276**, 2104 (2004)
29. Anwar, M.S., Kumar, S., Ahmed, F., Arshi, N., Kim, G.W., Koo, B.H.: J. Korean Phys. Soc. **60**, 1587 (2012)